Electronic Supplementary Material (ESI) for Journal of Materials Chemistry A.
This journal is © The Royal Society of Chemistry 2019

Supporting Information

Surface & Grain Boundaries Co-passivation by Fluorocarbon based Bifunctional Molecules for Perovskite Solar Cells with Efficiency Over 21%

Pengfei Guo, Qian Ye*, Xiaokun Yang, Jin Zhang, Fei Xu, Dmitry Shchukin, Bingqing Wei, Hongqiang Wang*

Mr. P. Guo, Dr. Q. Ye, Mr. X. Yang, Ms. J. Zhang, Dr. F. Xu, Prof. B. Wei, Prof. H. Wang
State Key Laboratory of Solidification Processing, Center for Nano Energy Materials, School of Materials Science and Engineering, Northwestern Polytechnical University and Shaanxi Joint Laboratory of Graphene (NPU), Xi'an, 710072, P. R. China
Dr. Q. Ye
Research & Development Institute of Northwestern Polytechnical University in Shenzhen, Northwestern Polytechnical University, Xi'an, 710072, P. R. China
Prof. D. Shchukin,
Stephenson Institute for Renewable Energy, Department of Chemistry, University of Liverpool, Crown Street, Liverpool, L69 7ZD, United Kingdom
Prof. B. Wei
Department of Mechanical Engineering, University of Delaware, Newark, Delaware 19716, United States
Prof. Q. Meng

Email: yeqian213@nwpu.edu.cn; hongqiang.wang@nwpu.edu.cn

Experimental

Materials

Unless stated otherwise, all materials were purchased from Sigma-Aldrich and used as received. Fuorine-doped tin oxide (FTO) glass substrates (around 1.5 cm×1.5 cm) were obtained from Pilkington and etched by a commercial corporation. Spiro-OMeTAD (2,2',7,7'-Tetrakis[N,N-di(4-methoxyphenyl)amino]-9, 9'-spirobifuorene, ≥99.8% purity), 4-tert-butylpyridine (tBP, ≥99.9% purity) and lithium-bis(trifluoromethanesulfonyl)imide (Li–TFSI, ≥99.9% purity) were supplied by Xi'an Polymer Light Technology Corp. 1H,1H-Perfluorooctylamine (PFA, ≥99.9% purity) was bought from Alfa Aesar.

Device fabrication

The etched FTO substrates were cleaned sequentially in Hellmanex detergent, acetone and ethanol, isopropyl alcohol, dried with a compressed nitrogen gun, and finally treated under an oxygen plasma for 10 min to remove the last traces of organic residues. A ~50 nm thick TiO_2 compact layer was then spin-coated onto the FTO substrate at 2000 rpm for 60 s using an acidic titanium diisopropoxidebis (acetylacetonate) solution (75% in 2-propanol) diluted in ethanol (1:39, volume ratio) as the precursor, followed by drying at 150 °C for 10 min and annealing at 500 °C for 30 min in air.

Fabrication of perovskite films with surface & GBs co-passivation: (1) $MAPbI_3$. A 1.2 M $MAPbI_3$ precursor solution of PbI_2 (1.2 M) and MAI (1.2 M) was stirred in a mixture of DMF and DMSO (4:1 v/v) at 60 °C for 2 h; (2) $Cs_{0.05}FA_{0.81}MA_{0.14}PbI_{2.55}Br_{0.45}$. A1.2 M "mixed" perovskite precursor solutions containing CsI (0.06M) FAI (0.97 M), PbI_2 (0.97 M), MABr (0.17 M) and $PbBr_2$ (0.17M) was stirred in a mixture of DMF and DMSO (4:1 v/v) at 60 °C for 2 h. The resulting solution was coated onto the FTO/TiO_2 substrate in an argon glovebox by a consecutive two-step spin-coating process at 1,000 and 4,000 r.p.m for 10 and 30 s, respectively. During the second step, 200 μL PFA with different concentrations (0.6, 1.2, 2.4,

6.0 and 15 mg/mL) in chlorobenzene was immediately poured on the spinning substrate 10 s prior to the end of the program. Thereafter, the substrate was put onto a hotplate for 60 min at 100 °C, forming the $MAPbI_3$-molecule film and the $Cs_{0.05}FA_{0.81}MA_{0.14}PbI_{2.55}Br_{0.45}$- molecule film.

Fabrication of perovskite film with surface-only passivation: PFA solution with different concentrations (0.6, 1.2, 2.4, 6.0 and 15 mg/mL) in chlorobenzene was spin coated onto the preformed $MAPbI_3$ and $Cs_{0.05}FA_{0.81}MA_{0.14}PbI_{2.55}Br_{0.45}$ perovskite layer at 3000 rpm for 30 s followed by annealing at 70 °C for 10 min, forming the $MAPbI_3$/ molecule film and the $Cs_{0.05}FA_{0.81}MA_{0.14}PbI_{2.55}Br_{0.45}$/ molecule film.

Fabrication of perovskite film with PFA molecules in the precursors: the molecule was added into DMF with a concentration 6.0 mg/mL forming a DMF-molecule mixed solution. A 1.2 M $MAPbI_3$ precursor solution of PbI_2 (1.2 M) and MAI (1.2 M) was stirred in a mixture of DMF-molecule and DMSO (4:1 v/v) at 60 °C for 2 h forming the molecule involved $MAPbI_3$ film ($MAPbI_3$+ molecule).

After cooling down to room temperature, the HTM solution was then deposited by spin coating at 5,000 r.p.m. for 30 s. The HTM solution was prepared by dissolving 72.3 mg Spiro-MeOTAD, 28.8 mL tBP and 17.5 mL of a stock solution of 520 mg/mL Li-TFSI in acetonitrile in 1 mL chlorobenzene. The samples were then aged in a desiccator for ~12 hrs. Finally, the Au counter electrode was deposited by thermal evaporation. The active area of this electrode was 0.1 cm^2, which was calculated by a mask plate and further determined by an optical microscope.

Device characterization

Simulated AM 1.5G irradiation (100 mW cm^{-2}) was produced by a xenon-lamp-based solar simulator (Oriel 67005, 150 W Solar Simulator) for current density-voltage *(J-V)* measurements. The light intensity was calibrated by a silicon (Si) diode (Hamamatsu S1133) equipped with a Schott visible-colour glass filter (KG5 colour-filter). A Keithley 2420 Source-

Meter was used for *J-V* measurement. The scanning rate was 0.2V/s with no device preconditioning, such as light soaking or extended forward voltage biasing in the dark before starting the measurement. The dark *I-V* characteristics of the electron-only devices were measured by a Keithley 2420 source, and the trap density was caculated using a previous method[1]. For the steady-state output measurement, the solar cells were put under the simulated AM1.5-G, 1-sunillumination to record the photocurrent under the bias of 0.937 and 0.908 V. External quantum efficiency (EQE) curves were characterized with a Newport QE measurement kit by focusing a monochromatic beam of light onto the devices. The morphology and structure of the samples were characterized by a field emission SEM with an EDS detector (FEI Nova) and an atomic force microscope (AFM, Bruker Dimension Icon). Scanning Kelvin Probe Microscopy (SKPM) measurements were performed on an Asylum Research MFP-3D-Origin AFM using Au-coated Si conductive probes (HA_HR, NT-MDT). TEM was performed in combination with EDS by using an FEI Tecnai F30 equipped with a field emission gun (FEG) operated at 300 kV, a high angle annular dark field (HAADF) STEM detector, and an Oxford Instruments EDS detector with an ultra-thin window. Focused ion beam (FIB) was used to prepare the cross sections of perovskite devices. X-ray diffraction (XRD) spectra were recorded on a PANAlyticalX'pert PRO equipped with a diffracted beam monochromator, and a conventional cobalt target X-ray tube set to 40 kV and 30 mA. X-ray photoelectron spectroscopy (XPS) depth profile measurements were conducted on a PHI Versa Probe II XPS system equipped with a small spot X-ray beam, automated charge compensation, monatomic and cluster ion guns (Ar+, C60, Arcluster), heating/cooling stage and angle-resolved XPS. The FTIR spectra (4000 to 500 cm^{-1}) were recorded on a Jasco FT/IR-6100 FTIR. The absorption was measured using the ultraviolet-visible (UV-vis) spectrophotometer (Perkin-Elmer Lambda 35 UV-vis-NIR). The steady-state photoluminescence spectra were measured using pulse laser as an optical excitation source (wavelength: 470 nm, Horiba FluorologFL-3), and time-resolved photoluminescence (TRPL) experiments were simultaneously performed by exciting at 470 nm.

The contact angles were measured on a Data physics OCA-20 contact-angle system at ambient temperature. Electrochemical impedance spectroscopy (EIS) was executed on a homemade electrochemical workstation. The EIS was measured under illumination of AM1.5G simulated solar light (100 mW cm-2) at 0.8V in a frequency range of 10 Hz-1 MHz. Moisture-stability measurements were performed in a constant temperature & humidity incubator in dark.

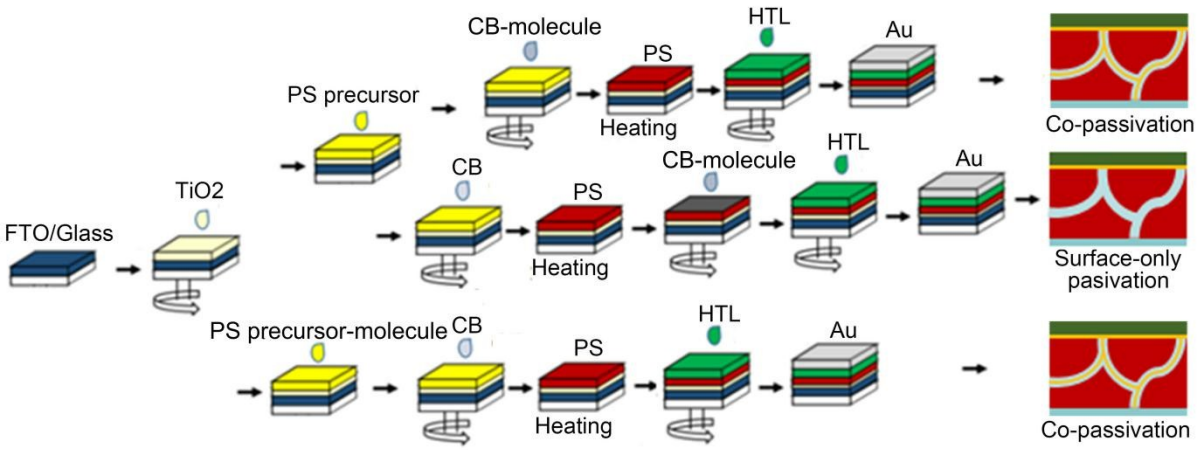

Scheme S1. Schematic illustration of the fabrication procedures for the Perovskite solar cells with different expected passivation: (A) Surface & GBs co-passivation; (B Surface-only passivation; (C) Surface & GBs co-passivation.

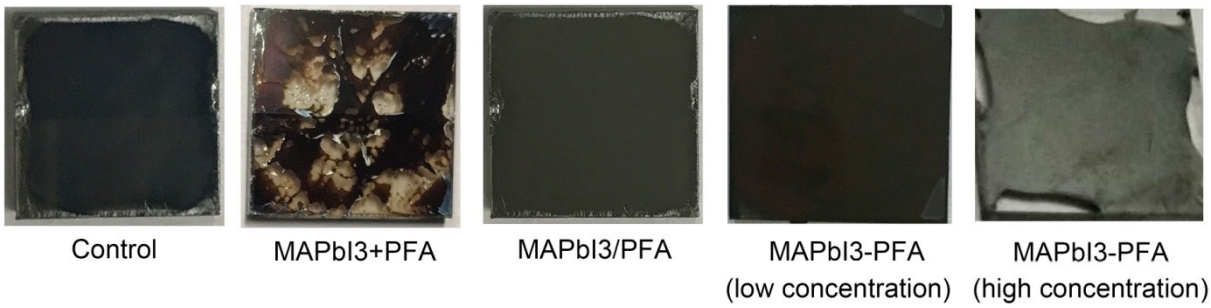

Figure S1 The optical images of different perovskite films: $MAPbI_3$ (control), $MAPbI_3$+PFA (adding into the precursor), $MAPbI_3$/PFA-4 (Surface-only passivation), $MAPbI_3$-PFA-4 (surface & GBs passivation), and $MAPbI_3$-PFA (50mg/ml in CB, surface & GBs passivation). The co-passivated film with a low concentration of PFA demonstrated continuous and complete coverage, while using of a higher concentration of PFA resulted in films with large pinholes and bad coverage.

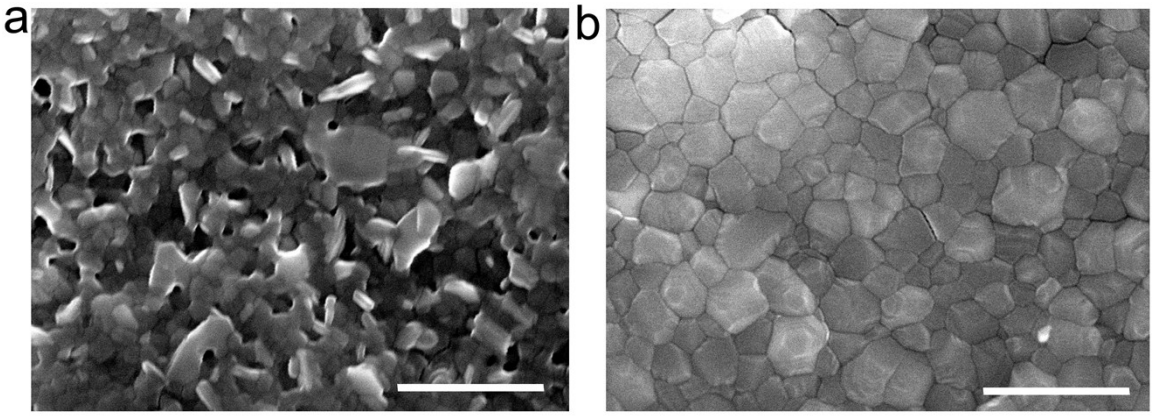

Figure S2 The SEM images of different perovskite films: **(a)** $MAPbI_3$+PFA-4 (adding PFA in precursors), **(b)** $MAPbI_3$ (control). The scale bar is 1 μm.

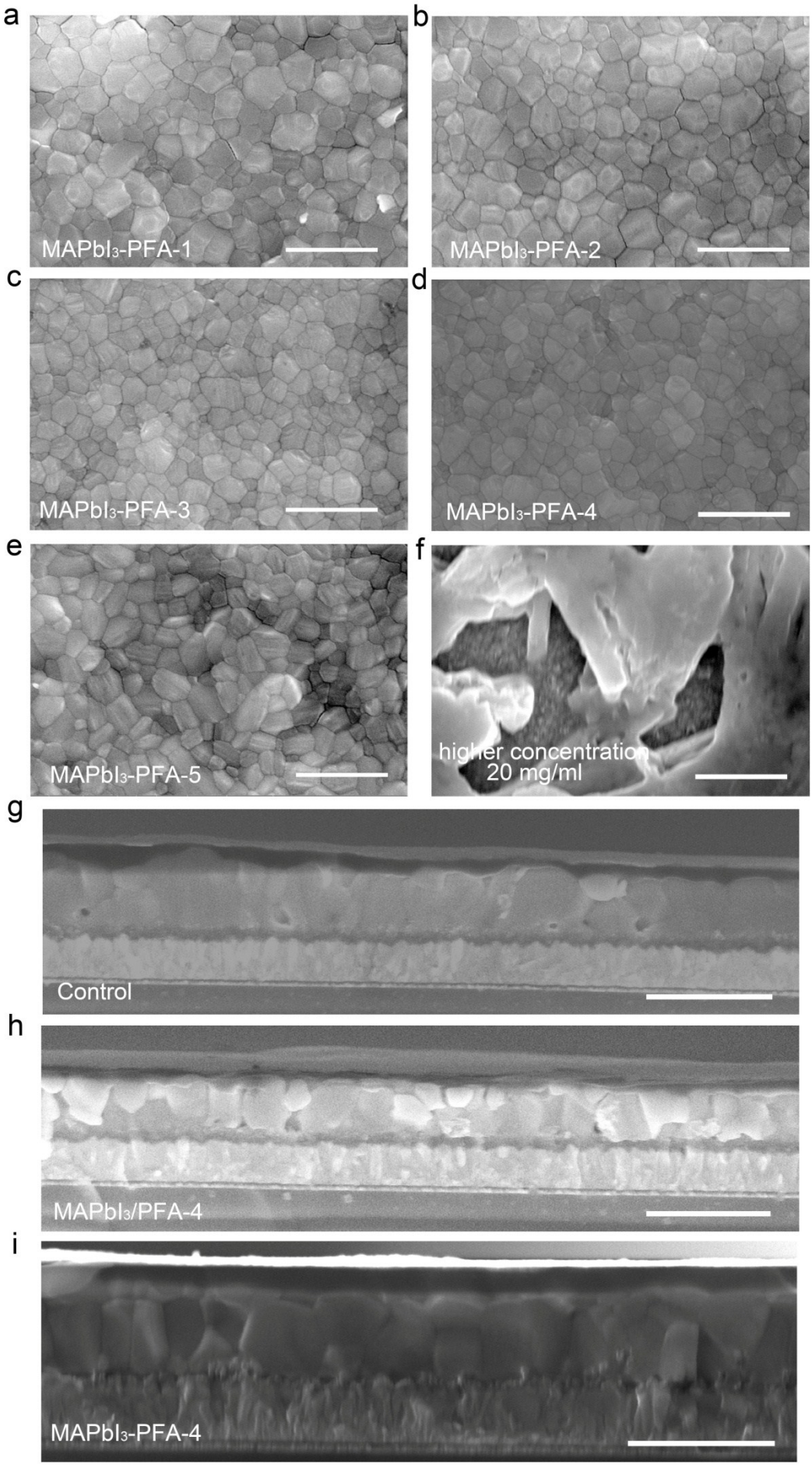
a
MAPbI3-PFA-1
b
MAPbI3-PFA-2
c
MAPbI3-PFA-3
d
MAPbI3-PFA-4
e
MAPbI3-PFA-5
f
higher concentration
20 mg/ml
g
Control
h
MAPbI3/PFA-4
i
MAPbI3-PFA-4

Figure S3 Surface morphologies of the co-passivated perovskite films with different PFA concentrations: **(a)** $MAPbI_3$-PFA-1, **(b)** $MAPbI_3$-PFA-2, **(c)** $MAPbI_3$-PFA-3, **(d)** $MAPbI_3$-PFA-4, **(e)** $MAPbI_3$-PFA-5, and **(f)** $MAPbI_3$-PFA with a high concentration ((20mg/ml in CB). Cross-sectional SEM images of different devices: **(g)** $MAPbI_3$ (control), **(h)** $MAPbI_3$/PFA-4 (surface-only passivation), and **(i)** $MAPbI_3$-PFA-4 (co-passivation). The scale bar is 1 μm. The co-passivated film with a low concentration of PFA (<6mg/ml in CB) has little influence on the morphological change comparing to the control film, while using a higher concentration of PFA (>20mg/ml in CB) resulted in films with large pinholes and bad coverage.

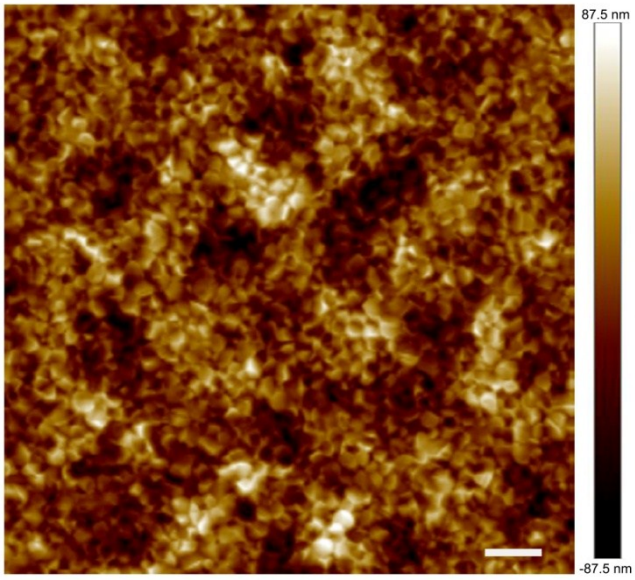

Figure S4 AFM image of the control film. The scale bar is 1 μm.

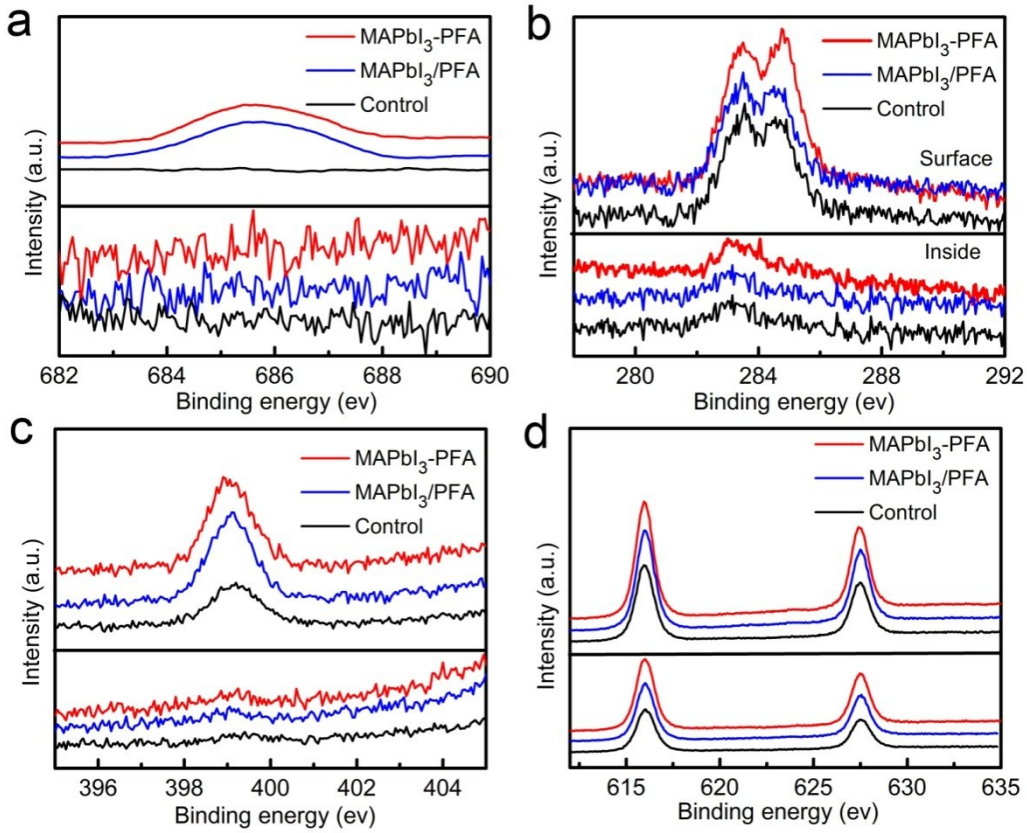

Figure S5 Binding energies of **(a)** F_{1s}, **(b)** N_{1s}, **(c)** C_{1s}, and **(d)** I_{3d} in surface and in-depth profile XPS spectra for the control ($MAPbI_3$), $MAPbI_3$-PFA, and $MAPbI_3$-PF films. The measured depth is about 20 nm (etch rate ≈ 0.1 nm/s, 200s).

As we assume that Routes A and C result in different distributions of PFA in the perovskite layer (see **Scheme S1**), X-ray photoelectron spectroscopy (XPS) was employed to experimentally verify the exact location of PFA in each resulted film. As shown in **Figure 1g**, the evident peak of F_{1s} located at around 685.7 eV can be found for both $MAPbI_3$-PFA and $MAPbI_3$/PFA films, illustrating the existence of PFA molecules on the surface of the both films. As we expect only the $MAPbI_3$-PFA film has PFA inside, XPS depth profile was further investigated to explore the depth distribution difference of F element between the two type films. However, signals of F_{1s} were not detected for both films. Detailed investigation reveals that signals of N_{1s} and C_{1s} have also been found in film surface but not inside, reflecting that the missed detection of F element deep in the $MAPbI_3$-PFA film might be due to the removing of light elements by the high energy Ar ion beam during the XPS depth profile characterization.

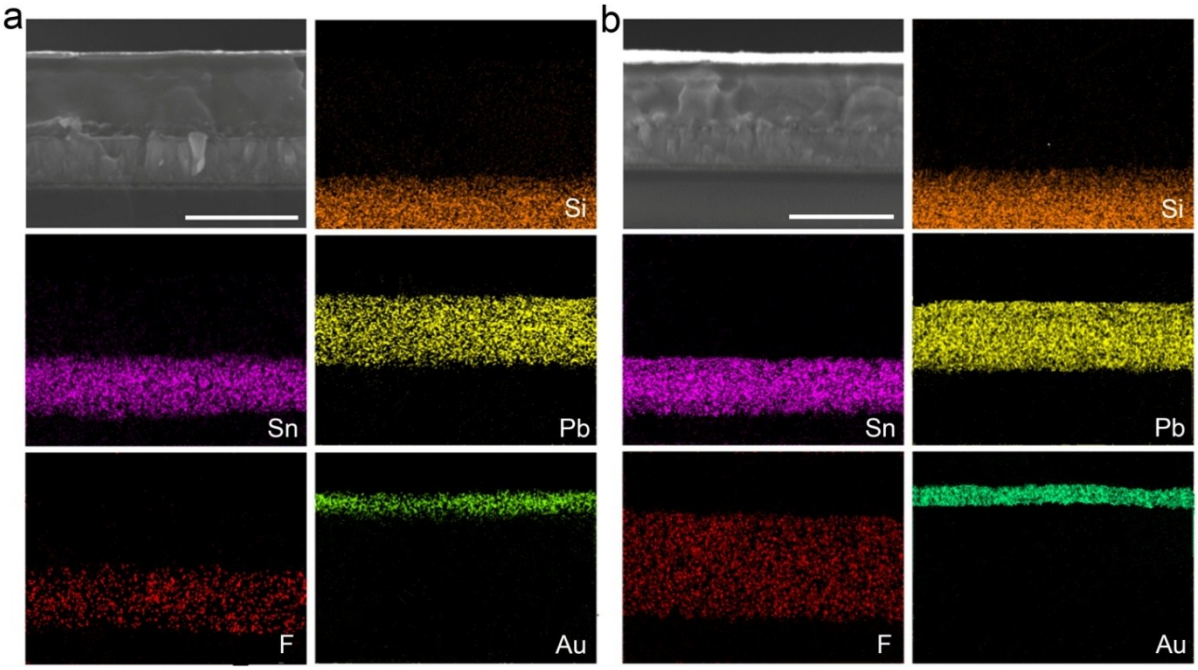

Figure S6 Cross-sectional SEM images and corresponding SEM-EDS mappings (Pb, F, and Sn) of **(a)** $MAPbI_3$/PFA and **(b)** $MAPbI_3$-PFA devices.

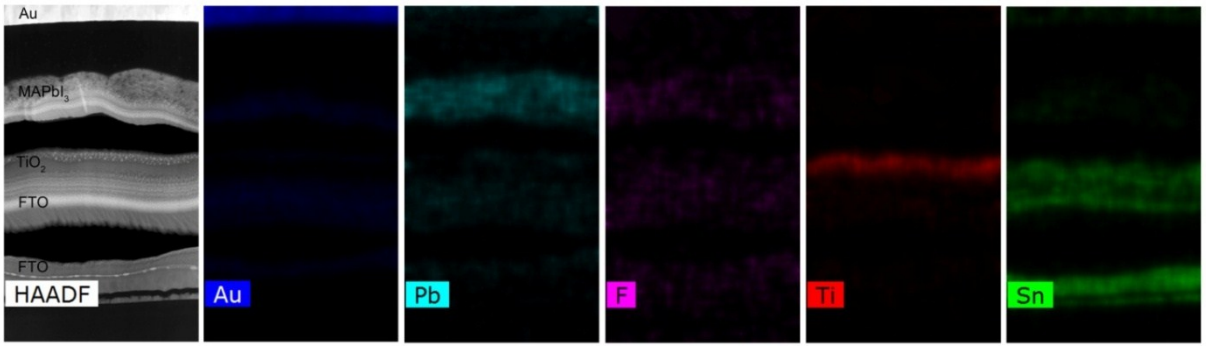

Figure S7 Cross-sectional HAADF image and EDS mapping of the $MAPbI_3$-PFA device, obtained from the FIB and the STEM mode.

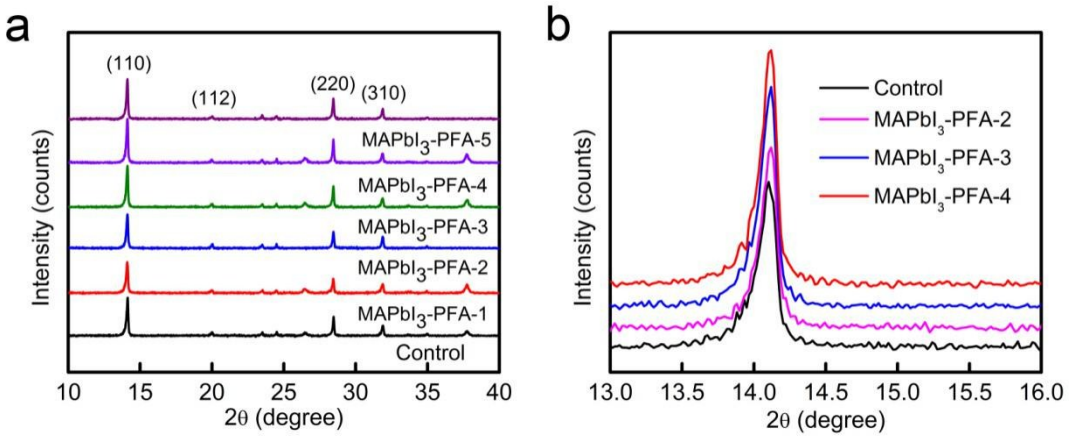

Figure S8 XRD patterns of co-passivated perovskite films with different concentrations: **(a)** 10-40°and **(b)** 13-16°

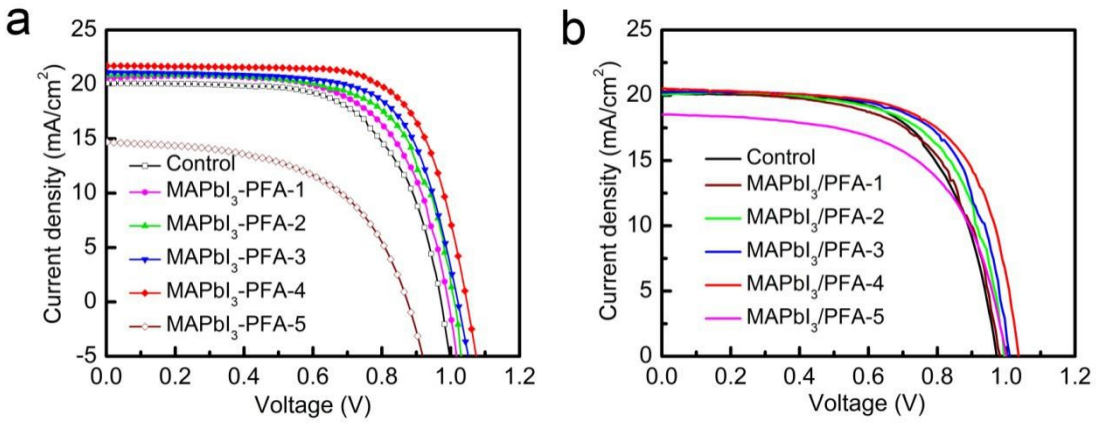

Figure S9 *J-V* curves of the champion PSCs for **(a)** $MAPbI_3$-PFA and **(b)** $MAPbI_3$/PFA with different concentrations.

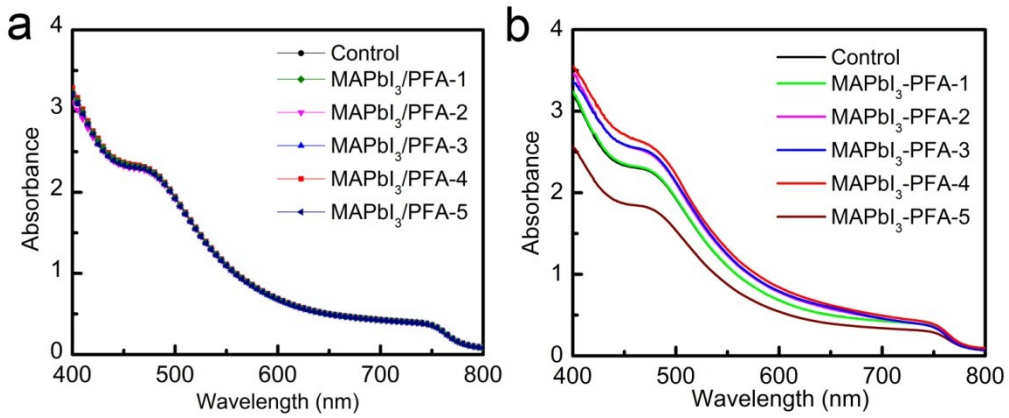

Figure S10 UV-Vis spectra of **(a)** $MAPbI_3$/PFA-4 films and **(b)** $MAPbI_3$-PFA films with different concentrations of PFA.

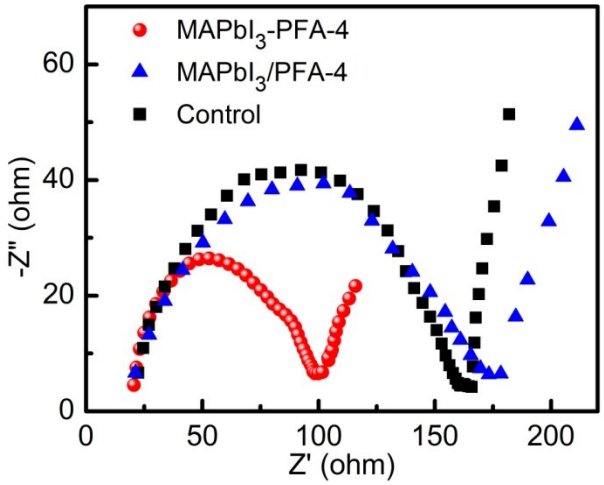

Figure S11 Nyquist plots of $MAPbI_3$, $MAPbI_3$/PFA-4 and $MAPbI_3$-PFA-4 devices measured at a bias of 0.8 V under simulated AM1.5 illumination.

The results from EIS reveal that the values of R_S are similar for these three devices, but the co-passivated device exhibits a much lower charge transfer resistance (95.2 Ω) than that of the control (1441.5) and surface-only passivated devices (149.7 Ω).

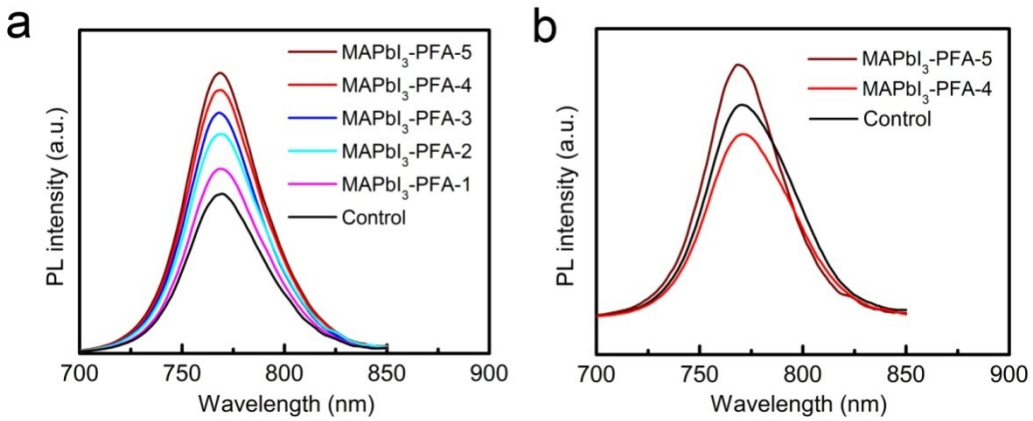

Figure S12 Steady-state PL spectra of **(a)** $MAPbI_3$-PFA and **(b)** $MAPbI_3$-PFA-HTL films with different concentrations of PFA.

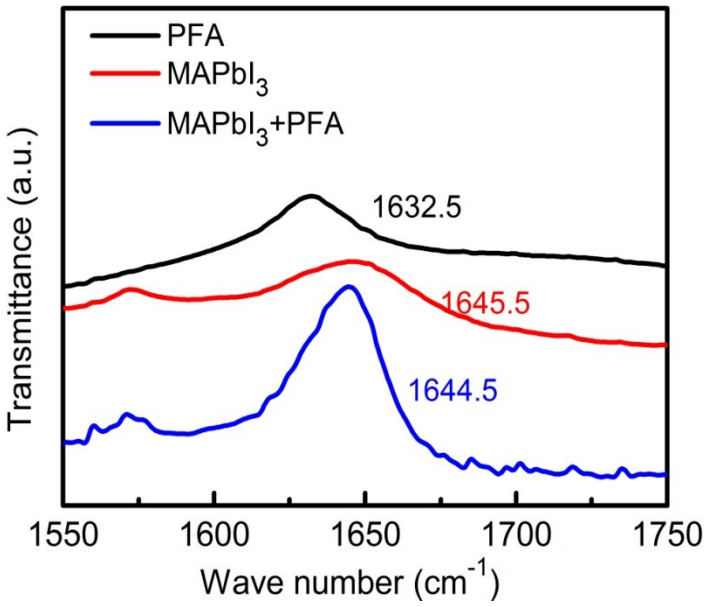

Figure S13 FTIR spectra of the PFA, $MAPbI_3$, and $MAPbI_3$+PFA films.

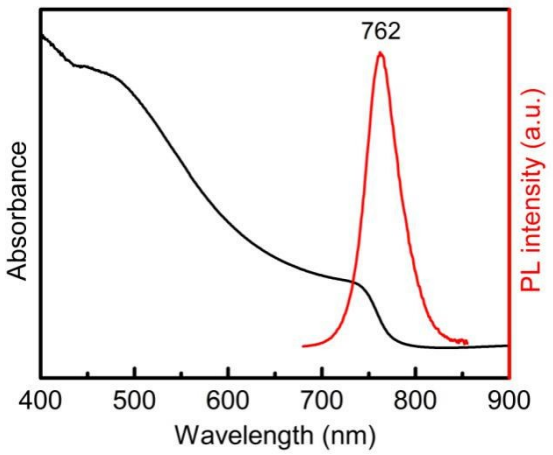

Figure S14 UV-Vis spectrum and steady-state PL spectrum of the CsFAMA film.

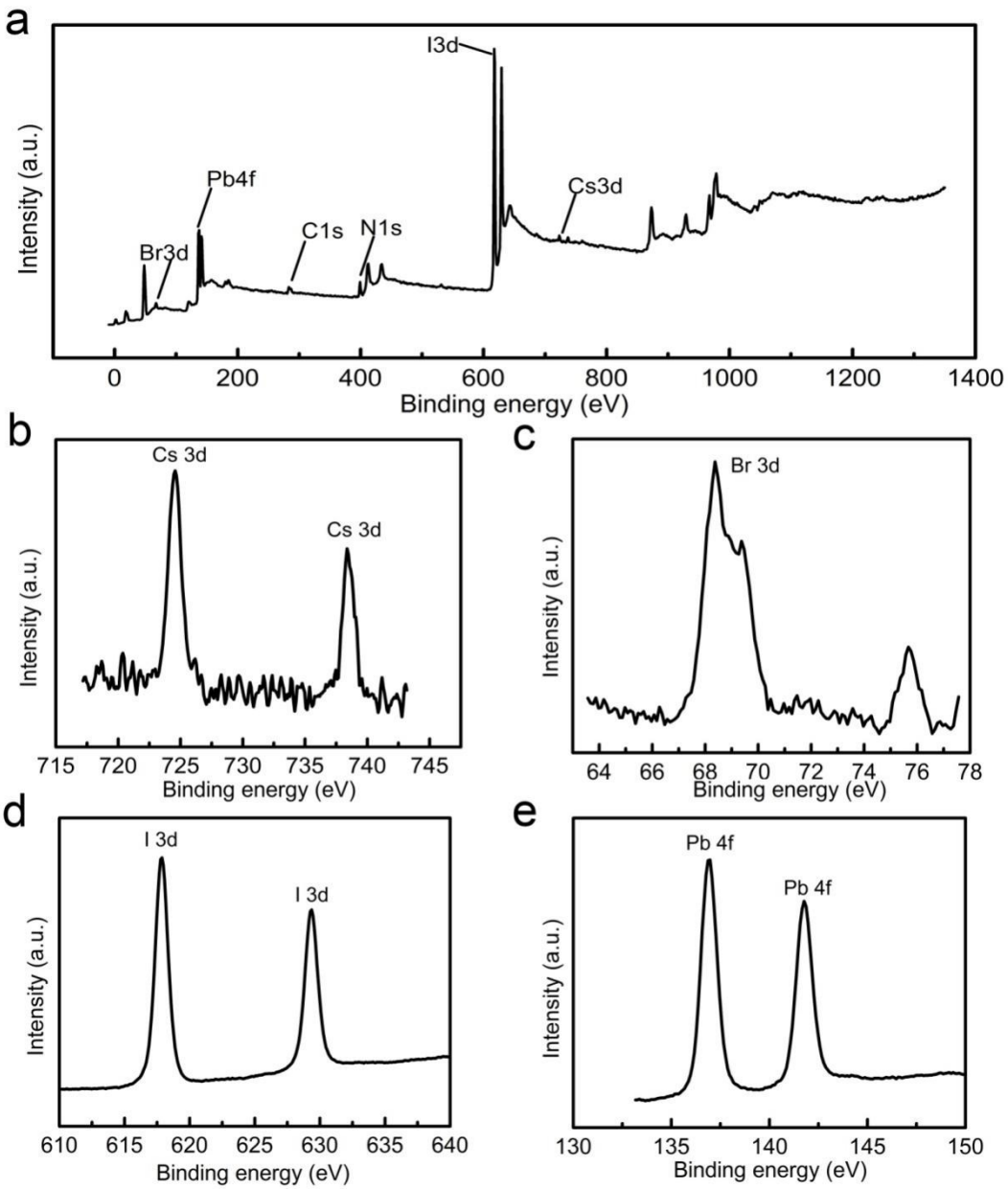

Figure S15 (a)XPS spectrum and binding energies of **(b)** Cs_{3d}, **(c)** Br_{3d}, **(d)** I_{3d}, and **(d)** Pb_{4f} of the CsFAMA-PFA film.

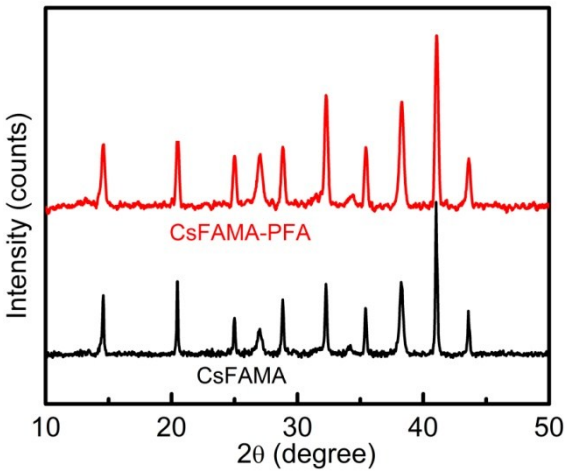

Figure S16 XRD patterns of the CsFAMA and CsFAMA-PFA films.

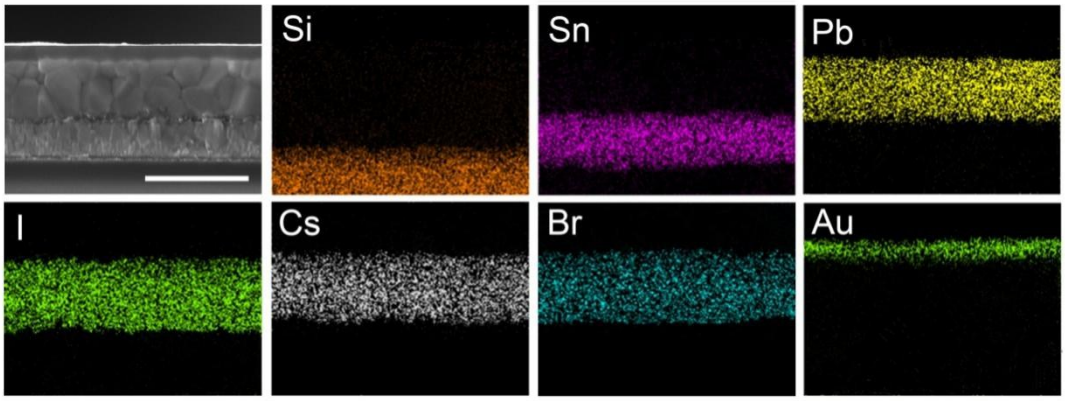

Figure S17 SEM-EDS mappings of Si, Sn, Pb, I, Cs, Br, and Au for a CsFAMA device. The scale bar is 1 μm.

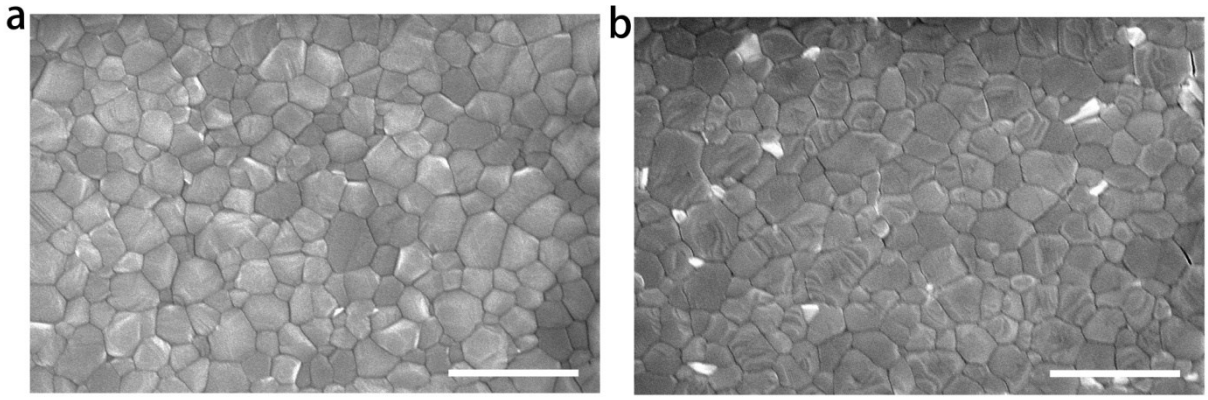

Figure S18 Surface morphologies of the CsFAMA (a) and the CsFAMA-PFA-4 (b) films.

The scale bar is 1 μm.

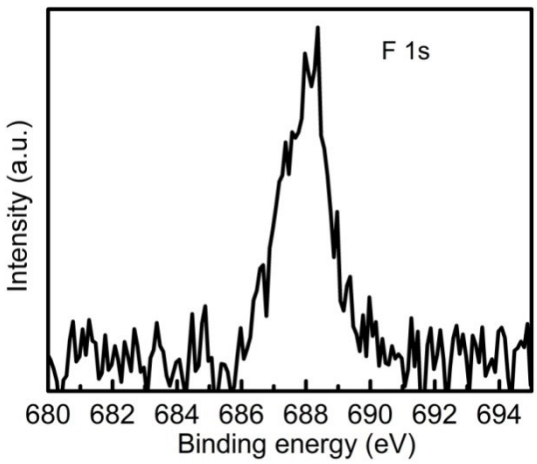

Figure S19 Binding energy of F_{1s} at the surface for the CsFAMA-PFA-4 film.

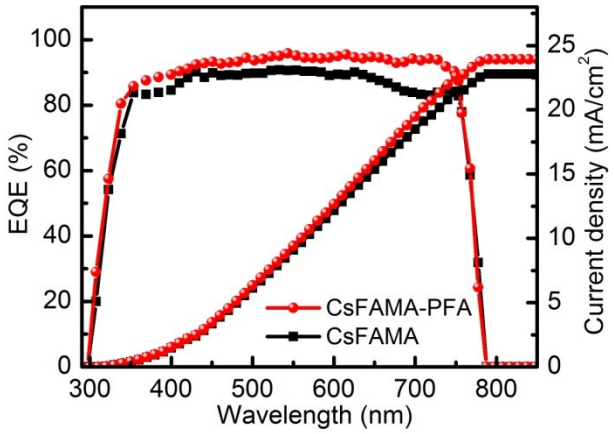

Figure S20 EQE spectra together with integrated J_{sc} for the CsFAMA-PFA and CsFAMA devices.

The EQE measurements indicate that co-passivation in CsFAMA based devices results in a broad plateaus with exceeding 90% along the whole absorption spectrum. The calculated integrated J_{sc} values are 22.77 and 23.93 mA/cm^2 for devices of CsFAMA, and co-passivation, respectively, which match well with the *J-V* measurements in **Figure 4g**.

Table S1 Summary of the best performance for the control, $MAPbI_3$-PFA-1, $MAPbI_3$-PFA-2, $MAPbI_3$-PFA-3, $MAPbI_3$-PFA-4, and $MAPbI_3$-PFA-5 cells. The scan rate is 0.2V/s.

Devices	Scan Direction	J_{sc} (mA cm^{-2})	V_{oc} (V)	FF (%)	Efficiency (%)
Control	Reverse	20.14	0.98	64.39	12.71
	Forward	20.14	0.95	45.37	8.68
$MAPbI_3$-PFA-1	Reverse	20.55	0.99	60.33	12.27
$MAPbI_3$-PFA-2	Reverse	20.92	1.01	67.08	14.17
$MAPbI_3$-PFA-3	Reverse	21.11	1.02	68.83	14.82
$MAPbI_3$-PFA-4	Reverse	21.71	1.05	70.97	16.18
	Forward	21.70	1.05	70.16	16.00
$MAPbI_3$-PFA-5	Reverse	14.84	0.87	54.45	7.01

Table S2 Summary of the best performance for the control, $MAPbI_3$/PFA-1, $MAPbI_3$/PFA-2, $MAPbI_3$/PFA-3, $MAPbI_3$/PFA-4, and $MAPbI_3$/PFA-5 cells. The scan rate is 0.2V/s.

Devices	Scan direction	J_{sc} (mA/cm^2)	V_{oc} (V)	FF (%)	Efficiency (%)
Control	Reverse	20.14	0.98	64.39	12.71
	Forward	20.14	0.95	45.37	8.68
$MAPbI_3$/PFA-1	Reverse	20.31	0.98	64.74	12.89
$MAPbI_3$/PFA-2	Reverse	20.23	0.99	65.72	13.16
$MAPbI_3$/PFA-3	Reverse	20.20	1.01	67.08	13.69
$MAPbI_3$/PFA-4	Reverse	20.45	1.04	68.10	14.48
	Forward	20.52	1.02	65.86	13.78
$MAPbI_3$/PFA-5	Reverse	18.50	1.00	60.18	11.12

Table S3 Fast PL lifetime (τ_1), slow PL lifetime (τ_2), and average lifetime (τ_{avg}) for the control, surface-only passivation, and co-passivation films.

Passivation Route	τ_1 (ns)	A_1 (%)	τ_2 (ns)	A_2 (%)	τ_{avg} (ns)
Co-passivation	23.7	26	121.2	74	95.85
Surface-only passivation	18.3	34	102.7	65	72.98
Control	2.9	54	17.8	46	9.75

Table S4 Photovoltaic parameters of perovskite devices before and after co-passivation.

Sample	Scan direction	J_{SC} (mA/cm^2)	V_{OC} (V)	FF (%)	Champion PCE (%)
Control	Forward	23.42	1.09	64.55	16.48
	Reverse	23.42	1.11	75.16	19.53
Co-passivation	Forward	24.06	1.13	78.26	21.28
	Reverse	24.10	1.14	77.56	21.31

Supporting References:

[1] Q. Dong, Y. Fang, Y. Shao, P. Mulligan, J. Qiu, L. Cao, J. Huang, *Science* **2015**, *347*, 967.